RSC Advances

ROYAL SOCIETY OF CHEMISTRY

www.rsc.org/advances

Dynamic Article Links ►

Cite this: DOI: 10.1039/c0xx00000x

www.rsc.org/xxxxxx

ARTICLE TYPE

Honeycomb porous films of pentablock copolymer on liquid substrates *via* breath figure method and their hydrophobic properties with static and dynamic behaviour

Zhiguang Li,[a,b] **Xiaoyan Ma,***[a,b] **Duyang Zang,**[a] **Qing Hong**[a,b] **and Xinghua Guan**[a,b]

Received (in XXX, XXX) Xth XXXXXXXXX 20XX, Accepted Xth XXXXXXXXX 20XX
DOI: 10.1039/b000000x

Amphiphilic pentablock copolymer of poly (trifluoroethyl methacrylate)-*b*-poly (methyl methacrylate)-*b*-poly (ethylene glycol)-*b*-poly (methyl methacrylate)-*b*-poly (trifluoroethyl methacrylate) (PTFEMA-*b*-PMMA-*b*-PEG-*b*-PMMA-*b*-PTFEMA) was proposed to fabricate honeycomb porous films on various liquid substrates through breath figure method. This work reported an investigation on the morphologies of the pores on different liquid substrates, and discussed the hydrophobic properties of the films with different surface morphologies. The morphologies of the films prepared on the solid substrate of silicon wafer and liquid substrate of methyl silicone oil were compared, and found that the pore size was larger and regularity was lower on the methyl silicone oil substrate. It was noteworthy that the surface thermodynamics was the important influence factor for the porous structures formation. In addition, the porous structures prepared on various liquid substrates were related to the surface tensions and viscosities of the liquid solvents. The pore size was increased by enhancing the surface tension of the liquid solvent. In addition, an increase in the viscosity leads to an increase in the pore size. Finally, the hydrophobic properties including wettability and water droplet impact behaviour of porous and pincushion structures films with different surface morphologies obtained from the liquids substrates were also investigated. Moreover, the water droplets exhibited different dynamic evolutions after impact on the flat, porous and peeled surfaces.

1. Introduction

The Honeycomb ordered porous films have attracted considerable interest because of their outstanding properties such as large surface area and high porosity, which make them suitable for a wide range of high technology applications such as separation membranes, superhydrophobic surfaces, cell culture and catalysis.[1-6] It has been reported that porous films can be prepared by breath figure (BF) method, which is a promising efficient, simple, and inexpensive technique to create highly ordered honeycomb films.[7, 8] As a dynamic templating method for film-forming materials, the BF technique can dynamically control the morphology of the resultant pores.[9-11]

In this technique, the rapidly evaporation of the solvent results in the temperature gradient between humid atmosphere and casting solution, which causes the water condense onto the solution surface. Influenced by the capillary force and Marangoni convection, the condensed water droplets rearrange into a hexagonal array, where the polymer precipitates, encapsulating the water droplets and preventing their coalescence.[12] The complete evaporation of both solvent and water results in the film with a strictly ordered array of honeycomb holes.[13] As shown in previous studies, the morphology of the porous film can be significantly affected by various critical factors such as polymer structures, concentration of the casting solution, relative humidity as well as substrate,[13, 14] and tiny changes in the influence factors may lead to obviously diverse porous structures. In all these cases, substrate must be taken into account as partially responsible for this phenomenon.[15]

It is known that the surface properties of the substrate have been demonstrated to have a great impact on the morphologies of copolymer films,[16-18] and different substrates may lead to films with various patterns and structures such as hexagonal or square arrays, through-pores and the regularity of the pores in the literature until now,[15, 19-22] An earlier study by Xi *et al.*[23] revealed that mica was the best surface for the casting of dendronized block copolymers, while the other surfaces such as glass and silicon plates couldn't form regularity arrays. Similar results have been obtained by Billon *et al.*[15] Moreover, Ferrari's group[21] found that the properties of interfaces can play an important role both for the pore size and regularity, and they suggested a possible mechanism that qualitatively accounts for hydrophilicity, wettability and polymer characteristics. In addition, Wan *et al.*[19] fabricated highly ordered honeycomb films with through-pores on the surfaces of ice and other organic solvents including glycerol and formic acid. Thus, how the substrate influences the morphologies of the porous films is complex, and even more to the complex polymer structures and liquid substrates.

Generally, the surface hydrophobic property strongly depends on the chemical composition and topology of the surface.[24-26] Recently, the control of surface morphology has received considerable attention because of the need for enhanced wettability of surfaces.[6] The preparation of these surfaces has relied by the introduction of particular surface morphologies with rough structures and surface modification. To our knowledge, the honeycomb films prepared through BF method is a good candidate for controlling surface chemistry and topology to obtain hydrophobic surfaces.[5, 27-30] Moreover, the top layer of porous film can be very easily peeled off, exposing a pincushion structure with even higher roughness which exhibits superhydrophobic properties. In addition, the hydrophobic property can also be measured by the water droplet impact behaviour. When a droplet is allowed to free fall and hit a surface, it can stick, spread or bounce. In practical on superhydrophobic surface, it should maintain its ability to repel penetrating droplets under the dynamic conditions.[31, 32]

In present work, the pentablock copolymer of PTFEMA-*b*-PMMA-*b*-PEG-*b*-PMMA-*b*-PTFEMA was chosen as film-forming material to explore the influence of surface thermodynamics to the surface morphologies and their hydrophobic properties. Based on our preliminary work,[33] the effect of liquid substrates with different surface tension and viscosity on the morphologies were investigated. In addition, the surface hydrophobic properties including wettability and water droplet impact behaviour of the films with different morphologies such as flat, porous and peeled films were tested, which have not been systemically investigated previously.

2. Experimental

2.1. Materials

The pentablock copolymer of PTFEMA-*b*-PMMA-*b*-PEG-*b*-PMMA-*b*-PTFEMA (M_n=26790g/mol, PDI=1.49) was synthesized through atom transfer radical polymerization in our previous study.[33] Water used in all experiments was de-ionized and ultrafiltrated to 18.2MΩ with an ELGA Labwater system. All other reagents (chloroform, glycerol, formic acid, ethylene glycol, ethyl acetate, ethanol, isopropanol, methanol, the methyl silicone oil) were analytical grade and used without further purification.

2.2. Preparation of honeycomb films

The honeycomb porous films were prepared through BF method. To prepare ordered porous films, 45mg/mL of the pentablock copolymer was dissolved in chloroform, and then caste onto solid substrate (silicon wafer) and liquid substrates (methyl silicone oil, water, glycerol, formic acid, ethylene glycol, ethyl acetate, ethanol, isopropanol and methanol) under a humid airflow. The airflow was vertically blown over the solution surface. The solvent started to evaporate and water vapor condensed onto the solution surface simultaneously. After complete evaporation of the solvent and water, the ordered porous films were prepared. For compression, nonporous film of the pentablock copolymer on the surfaces of silicon wafer or methyl silicone oil was cast and dried under normal conditions.

2.3. Water droplet impact dynamics monitor

The water droplet with volume of 10μL was generated using a micro-syringe and allowed to free fall at a certain height and impact on the flat, porous and peeled surfaces with different morphologies. The impact velocity V_i was controlled by its falling height. The process of the droplet impact behaviour was recorded using a high speed camera Trouble Shooter HR (US) at a frame rate of 2000 fps for each experiment and then measuring the dynamic impact behaviour of the droplet as a function of time. The image data was analyzed using MaxTRAQ software.

2.4. Characterization

Scanning Electron Microscope (SEM) images were used to observe apparent morphologies of porous films, which were carried on VEGA 3 LMH (Česko TESCAN) with an accelerating voltage of 10 kV. The quantitative analysis was using energy-dispersive spectrometry (EDS) (Oxford INCA X-ACT). Contact angle measurements were measured by pendent drop method with a JC2000D4 Powereach Tensionmeter made by Shanghai Zhongchen Company. The copolymer solutions were cast on glass slides and the wetting liquid used was water. A microsyringe was used to deliver water to the film surface. For each angle reported, at least ten sample readings from different surface locations were averaged.

3. Results and discussion

3.1 Liquid substrates contribute to the honeycomb porous films

It is noteworthy that the substrates strongly influence the film morphologies in the BF method.[22, 34] Until now, the liquid substrate is less investigated and still missing due to its surface thermodynamics.[19] To explore the air/liquid interfaces on the formation of the porous films, we compared the solid substrate of silicon wafer and liquid substrate of methyl silicone oil. The SEM images of the films prepared on the two substrates as depicted in Fig. 1(a) and (b).

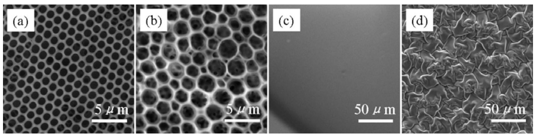

Fig. 1 SEM images of the films prepared on the two substrates: (a) and (c) silicon wafer, (b) and (d) methyl silicone oil. (a) and (b) BF method, (c) and (d) dried under normal conditions.

As evidenced in Fig. 1(a) and (b), the film obtained from the two substrates are different obviously. It is found that the pore structures exhibit regular arrays and high organizations on the silicon wafer substrate with uniform pore sizes of 0.94μm, while the pore patterns produced on the substrate of methyl silicone oil are less ordered, with non-uniform pore sizes between 1.19 and 2.61μm. Generally, in order to successfully explain the film formation on the two substrates, the solvent of the copolymer solution volatilized under normal conditions are investigated. The SEM images are exhibited in Fig. 1(c) and (d), and it is found that the silicon wafer substrate can form flat film while the methyl silicone oil substrate makes wrinkle formation, which is result from the surface thermodynamics. Herein, it turns out less ordered patterns in the BF method. The methyl silicone oil may restrain the spreading behaviour of copolymer solutions by slowing the nucleation of water droplets on the chloroform surface, which accordingly yields larger pore sizes.[20] On the other hand, the copolymer solution is prone to spread on the silicon wafer in our previous studies,[33] and form flat film in the normal volatilized conditions. As a result, the pore size is smaller on the silicon wafer than on the methyl silicone oil substrate, and the pore structure is regularity.

Recently, Wan *et al.*[19] investigated that through-pore films can be fabricated on the substrates of organic solvents with high surface tension and high density, and vice versa. However, how the substrate of organic solvents influence the surface morphologies is still missing, and no define conclusions can be drawn. Herein, we investigate the film morphologies prepared from different liquid substrates, and the SEM images are shown in Fig. 2. It is found that the pore structures are different, which may be correlated with the different spreading behaviours of the copolymer solutions on the substrates. The condition for spreading a drop of copolymer solution over a liquid substrate is determined by the surface thermodynamics, which can be described using a spreading coefficient S:[35]

$$S = \gamma_{sg} - \left(\gamma_{pg} + \gamma_{ps}\right) \qquad (1)$$

where γ_{sg} is the surface tension of the liquid surface; γ_{pg} is the surface tension of copolymer solution; and γ_{ps} is the interfacial tension between the copolymer solution and the liquid surface. $S \geq 0$ means complete wetting whereas $S < 0$ indicates partial wetting. Obviously, liquid surface with large surface tension will be beneficial to the spreading of copolymer solution by fasting the nucleation of water droplets, which leads to the small pore sizes.[36]

As depicted in Fig. 2, pore sizes of (a)-(d) are small which result from the higher spreading coefficient (S>0), while the pore sizes of (e)-(h) are large due to their lower spreading coefficient (S<0) (Table 1). Additionally, the pore sizes of (a)-(d) and (e)-(h) are related to the liquid surface's viscosity, and the pore size increased almost correspond to the enhancing of the liquid surface's viscosity.[33] For example, it is noteworthy that the pore size of the film prepared on the formic acid substrate is smaller than on the ethylene glycol substrate which corresponds to the enhancing of the liquid's viscosity. Herein, the pore size of the film on the isopropanol substrate is larger than on the ethanol substrate.

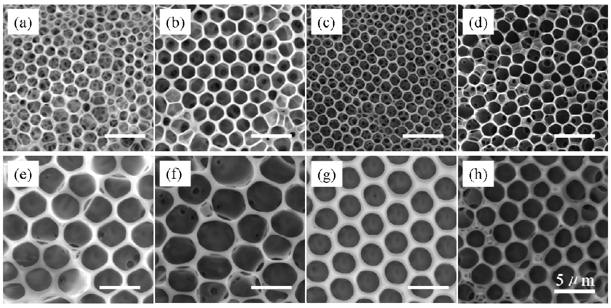

Fig. 2 SEM images of porous films prepared on different liquid substrates: (a) water, (b) glycerol, (c) formic acid, (d) ethylene glycol, (e) ethanol, (f) isopropanol, (g) ethyl acetate and (h) methanol.

Table 1. The surface tension, viscosity and spreading coefficient of the water and organic solvents

surfaces	water	glycerol	formic acid	ethylene glycol	ethanol	isopropanol	ethyl acetate	methanol
Surface tension, mN/m	72.4	63.3	35.8	46.5	21.0	22.0	26.3	24.0
Viscosity, mPa·s	1.00	243.00	1.96	25.66	1.20	2.43	0.45	0.60
Spreading coefficient, mN/m	13.1	36.8	9.1	20.0	-5.5	-4.5	-0.2	-2.5

3.2 Hydrophobic properties of the films with various surface morphologies

It is obvious that the wettability of the porous films can be influenced by the surface chemistry and surface roughness.[25, 37] Copolymers composed of fluorinate acrylate have proven to possess excellent hydrophobic property.[33] In this paper, the wettability of the porous films obtained on different liquids substrates of formic acid, ethylene glycol, ethanol and isopropanol are investigated. The pentablock copolymer has large hydrophobic segments and fluorine segments which enhance the hydrophobic property of the films. The surface fluorinate contents of the four porous films are 34.53%, 34.61%, 34.26% and 34.36% which are measured by EDS (Fig. S1), respectively, and also the carbon (17.72%, 17.25%, 18.64% and 17.70%) and oxygen (47.75%, 48.14%, 47.10% and 47.94%) contents (Table S1). It is found that the chemical compositions of the films are roughly the same. The higher fluorinate content influences the hydrophobic property.

Previous reports have suggested that the pore size/rim width (D/W) ratio can be correlated to the surface roughness and water contact angle; specifically, a high D/W ratio generally indicates a high water contact angle.[4, 24] In this paper, the D/W ratios of the porous films obtained on the liquids substrates of formic acid, ethylene glycol, ethanol and isopropanol are illustrated in Fig. 3. It is evident that the film on the isopropanol substrate has highest D/W ratio, due to the presence of relatively more roughness on the surface.

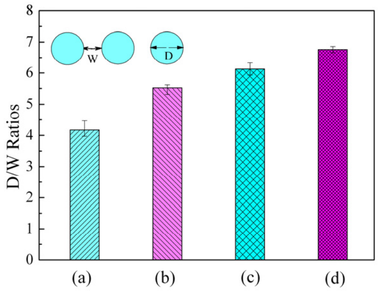

Fig. 3 The D/W ratios of the porous films obtained on different liquid substrates. (a) formic acid, (b) ethylene glycol, (c) ethanol and (d) isopropanol.

To further investigate the surface topography, the top layer of the porous films is peeled off using an adhesive tape to obtain a pincushion structure.[38] The wettability of the porous and peeled films measured by the contact angles are illustrated in Table 2. With respect to the water contact angle of 95.9° on flat film, these porous films present enhanced hydrophobic property, with their water contact angle reaching to 116.3°, 119.2°, 125.3° and 131.7°

on the substrates of formic acid, ethylene glycol, ethanol and isopropanol, respectively. The enhanced hydrophobic property is due to the increase of the D/W ratios as mentioned above, which create a more roughness.[39, 40] In addition, it is clearly shown that the peeled films with pincushion structure raise the water contact angles to 138.2°, 147.1°, 154.9° and 157.4°, respectively. The porous and peeled films enhance the surface roughness and amplify the hydrophobic properties.[5, 15]

Table 2. Contact angles (CA) on the porous and peeled films obtained on the four substrates

substrates	formic acid	ethylene glycol	ethanol	isopropanol
CA on porous films, °	116.3±1.9	119.2±2.3	125.3±2.1	131.7±1.8
CA on peeled films, °	138.2±2.5	147.1±3.4	154.9±2.6	158.4±3.1

The relationship between the rough topography and the water contact angle can be illustrated by the Cassie-Baxter law:[41, 42]

$$\cos\theta_r = f_1\cos\theta - f_2 \qquad (2)$$

where f_1 and f_2 are the fractions of the contact area of water droplets with solid and air ($f_1 + f_2 = 1$), respectively. θ_r and θ are the contact angles of the rough surface and flat surface, respectively.

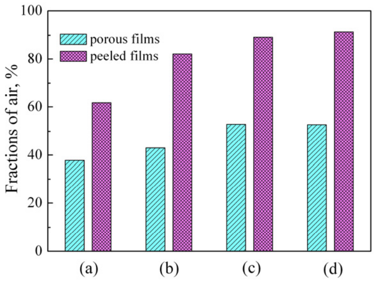

Fig. 4 Fractions of the airs on the porous and peeled films of (a) formic acid, (b) ethylene glycol, (c) ethanol and (d) isopropanol.

The fractions of the air on the porous and peeled films are depicted in Fig. 4. It is found that the peeled films have higher f_2 than porous films, and the higher D/W ratios of the porous film also have higher f_2. We learn that higher f_2 results in larger water contact angle and prevents water penetrating into the copolymer-based composite matrix.

To further explore the effect of surface morphologies on the hydrophobic properties, the water droplet impact behaviour is also explored on these surfaces.[31, 43, 44] Fig. 5 illustrates the morphology evolution of the water droplets after impact on different flat, porous and peeled surfaces from (a) to (e) with the static contact angles of 95.9°, 119.2°, 131.7°, 147.1° and 158.4°, respectively.

As depicted in Fig. 5, the water droplet with its initial spherical shape flattens into a pancake-like shape that stretched out over the surface at 5ms, and remains completely intact during the impact. It deforms and spreads rapidly upon impact, and then, the droplet moves back toward the centre after the time of maximum spread. It remains fastened onto the surface and pulsates violently. Finally, the droplet has a low contact angle on the flat surface (Fig. 5a). In contrast as shown in Fig. 5(b)–(e), the droplet shows different impact behaviour on the porous and peeled surfaces. Over time, the droplet finally reaches an equilibrium state, and the contact angles of final state are increased from (a)-(e).

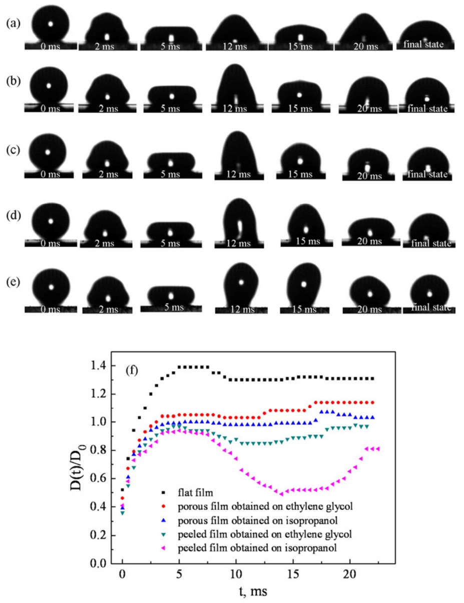

Fig. 5 Dynamics of water droplets impacting on the flat, porous and peeled surfaces. The volume of droplet is 10μL and impact velocity $V_i\approx$ 0.2m/s. (a) flat film, (b) and (c) porous films obtained from ethylene glycol and isopropanol substrates, respectively, (d) and (e) peeled films obtained from ethylene glycol and isopropanol substrates, respectively. (f) Time evolution of nondimensional contact diameter of the droplets scaled by the initial diameter before impact of (a)-(e).

Although the rebounding tendency of droplet becomes more and more obvious with increasing contact angle, the wetting adhesion is so intense that the droplet could not bounce off the surface after impact. In general, the droplet can rebound several times from the superhydrophobic surface.[31, 32] However, it could not bounce off on the superhydrophobic surface in Fig. 5(e). That is because the films exhibit excellent water-adhesion ability in our previous study.[33] Moreover, the resulting increase in spreading of the droplet significantly increases the adhesion (due to van der Waals forces) to the surface and prevents the contact area from retracting. The droplet is therefore unable to recover sufficient energy to rebound off the surface and as a consequence it simply vibrates on the surface.

In addition to the impact behaviour, the maximum spreading diameter of the droplet, D_{max}/D_0, is significantly weakened by the increased surface roughness (Fig. 5f), which is in agreement with the contact angle value and impact behaviour in Table 2 and Fig. 5. Moreover, the maximum D_{max}/D_0 values are immensely different, and decrease from 1.39 to 0.94 when the contact angles increase from 95.9° to 158.4° on these surfaces. Consequently, the droplets impact behaviour on these surfaces further indicates that the surface properties can be adjusted by tuning the surface morphologies, and the result suggests that the maximum spreading of droplets is determined by the surface wettability.

4. Conclusions

In this paper, the effects of liquid substrates on the surface morphologies of porous films and their hydrophobic properties are investigated through breath figure method. The surface thermodynamics plays extremely important role in determining the morphology and regularity of the honeycomb films. The pore size obtained on the methyl silicone oil substrate is larger than on the silicon wafer substrate, and the pore structures exhibit irregular arrays. Additionally, the surface tension and viscosity of the liquid substrate influence the pore morphologies, and the liquid substrates with higher surface tension and lower viscosity make the pore smaller.

The hydrophobic properties including wettability and water droplet impact behaviour on the surfaces with different morphologies are investigated. It is found that the pore morphologies influence the hydrophobic properties, and the pore size/rim width (D/W) ratios of the porous films are related to the hydrophobic properties. Herein, the porous film on the isopropanol substrate has highest D/W ratio result in best hydrophobic property. In addition, the peeled film has higher air fraction of the surface than porous film, which results in larger water contact angle. The dynamic wettability is also explored by analyzing the water droplet impact on the flat, porous and peeled surfaces. The rebounding tendency of droplet becomes more and more obvious and the maximum spreading diameter of the droplet is significantly weakened with increasing contact angle. It is noteworthy that the droplet can’t rebound from the superhydrophobic surface due to the particular peeled structure which exhibits excellent water-adhesion ability.

Acknowledgements

This work is supported by the National Natural Science Foundation of China (Grant No. 51372206, 51301139), Natural Science Foundation of Shaanxi Province (Grant No. 2013JM2012), Innovation Project of Science and Technology of Shaanxi Province (Grant No.2013KTCG01-14) and NPU Foundation for Fundamental Research (NPU-FFR-JCY20130147). Thanks for Wenxia Zhang for the water droplet impact behaviour experiment.

Notes

[a] *Key Laboratory of Space Applied Physics and Chemistry, Ministry of Education, Shaanxi province, School of Science, Northwestern Polytechnical University, Xi’ an 710129, China. Tel: +86-29-88431676; E-mail: m_xiao_yana@nwpu.edu.cn*

[b] *Key Laboratory of Polymer Science and Technology, Shaanxi province, School of Science, Northwestern Polytechnical University, Xi’an, 710129, China.*

References

1. C. Du, A. Zhang, H. Bai and L. Li, *ACS Macro Letters*, 2013, 2, 27-30.
2. X. Wu and S. Wang, *Polymer*, 2014, 55, 1756-1762.
3. L. Heng, R. Hu, S. Chen, M. Li, L. Jiang and B. Z. Tang, *Langmuir*, 2013, 29, 14947-14953.
4. X. Wu and S. Wang, *Acs Appl. Mater. Interfaces*, 2012, 4, 4966-4975.
5. P. Escale, W. Van Camp, F. Du Prez, L. Rubatat, L. Billon and M. Save, *Polym. Chem.*, 2013, 4, 4710-4717.
6. Y. Nakamichi, Y. Hirai, H. Yabu and M. Shimomura, *J. Mater. Chem.*, 2011, 21, 3884-3889.
7. H. Bai, C. Du, A. Zhang and L. Li, *Angew. Chem. Int.Ed.*, 2013, 52, 12240-12255.
8. U. H. F. Bunz, *Adv. Mater.*, 2006, 18, 973-989.
9. H. Ma, L. Kong, X. Guo and J. Hao, *RSC Adv.*, 2011, 1, 1187-1189.
10. X. Qiang, X. Ma, Z. Li and X. Hou, *Colloid Polym. Sci.*, 2014, 292, 1531-1544.
11. B.-B. Ke, L.-S. Wan, W.-X. Zhang and Z.-K. Xu, *Polymer*, 2010, 51, 2168-2176.
12. G. Widawski, M. Rawiso and B. Francois, *Nature*, 1994, 369, 387-389.
13. M. Srinivasarao, D. Collings, A. Philips and S. Patel, *Science*, 2001, 292, 79-83.
14. M. Hernández-Guerrero and M. H. Stenzel, *Polym. Chem.*, 2012, 3, 563-577.
15. L. Ghannam, M. Manguian, J. François and L. Billon, *Soft Matter*, 2007, 3, 1492-1499.
16. Z. Zhang, T. C. Hughes, P. A. Gurr, A. Blencowe, H. Uddin, X. Hao and G. G. Qiao, *Polymer*, 2013, 54, 4446-4454.
17. H. Ma, P. Gao, Y. Zhang, D. Fan, G. Li, B. Du and Q. Wei, *RSC Adv.*, 2013, 3, 25291-25295.
18. H. Battenbo, R. J. Cobley and S. P. Wilks, *Soft Matter*, 2011, 7, 10864-10873.
19. L.-S. Wan, J.-W. Li, B.-B. Ke and Z.-K. Xu, *J. Am. Chem. Soc.*, 2012, 134, 95-98.
20. J. Wang, H.-X. Shen, C.-F. Wang and S. Chen, *J. Mater. Chem.*, 2012, 22, 4089-4096.
21. E. Ferrari, P. Fabbri and F. Pilati, *Langmuir*, 2011, 27, 1874-1881.
22. C. Wang, Y. Mao, D. Wang, Q. Qu, G. Yang and X. Hu, *J. Mater. Chem.*, 2008, 18, 683-690.
23. C. X. Cheng, Y. Tian, Y. Q. Shi, R. P. Tang and F. Xi, *Langmuir*, 2005, 21, 6576-6581.
24. Y.-A. Su, W.-F. Chen, T.-Y. Juang, W.-H. Ting, T.-Y. Liu, C.-F. Hsieh, S. A. Dai and R.-J. Jeng, *Polymer*, 2014, 55, 1481-1490.
25. Y. Rahmawan, L. Xu and S. Yang, *J. Mater. Chem. A*, 2013, 1, 2955-2969.
26. L.-W. Zhu, W. Yang, Y. Ou, L.-S. Wan and Z.-K. Xu, *Polym. Chem.*, 2014, 5, 3666-3672.
27. P.-C. Chen, L.-S. Wan, B.-B. Ke and Z.-K. Xu, *Langmuir*, 2011, 27, 12597-12605.
28. J. Wang, C.-F. Wang, H.-X. Shen and S. Chen, *Chem. Commun.*, 2010, 46, 7376-7378.
29. A. S. de Leon, A. d. Campo, C. Labrugere, M. Fernandez-Garcia, A. Munoz-Bonilla and J. Rodriguez-Hernandez, *Polym. Chem.*, 2013, 4, 4024-4032.
30. L. Wang, S. H. Maruf, D. Maniglio and Y. Ding, *Polymer*, 2012, 53, 3749-3755.
31. D. Zang, F. Li, X. Geng, K. Lin and P. Clegg, *Eur. Phys. J. E*, 2013, 36, 1-8.
32. D. J. Lee, H. M. Kim, Y. S. Song and J. R. Youn, *ACS Nano*, 2012, 6, 7656-7664.
33. Z. Li, X. Ma, D. Zang, B. Shang, X. Qiang, Q. Hong and X. Guan, *RSC Adv.*, 2014, 4, 49655-49662.
34. A. Honglawan and S. Yang, *Soft Matter*, 2012, 8, 11897-11904.
35. L. Govor, I. Bashmakov, R. Kiebooms, V. Dyakonov and J. Parisi, *Adv. Mater.*, 2001, 13, 588-591.
36. L.-S. Wan, L.-W. Zhu, Y. Ou and Z.-K. Xu, *Chem. Commun.*, 2014, 50, 4024-4039.
37. M. V. Walter, P. Lundberg, D. Hult, A. Hult and M. Malkoch, *Polym. Chem.*, 2013, 4, 2680-2690.
38. Y.-C. Chiu, C.-C. Kuo, C.-J. Lin and W.-C. Chen, *Soft Matter*, 2011, 7, 9350-9358.
39. R. Dong, H. Ma, J. Yan, Y. Fang and J. Hao, *Chem–Eur.J.*, 2011, 17, 7674-7684.
40. W. Dong, Y. Zhou, D. Yan, Y. Mai, L. He and C. Jin, *Langmuir*, 2009, 25, 173-178.
41. B.-B. Ke, L.-S. Wan, P.-C. Chen, L.-Y. Zhang and Z.-K. Xu, *Langmuir*, 2010, 26, 15982-15988.
42. E. Bormashenko, S. Balter, A. Malkin and D. Aurbach, *Macromol. Mater. Eng.*, 2014, 299, 27-30.
43. W. Tian, L. Huang, D. Zang, C. Li, J. Dang and D. Wang, *RSC Adv.*, 2014, 4, 53021-53027.
44. J. B. Lee and S. H. Lee, *Langmuir*, 2011, 27, 6565-6573.

Graphical abstract

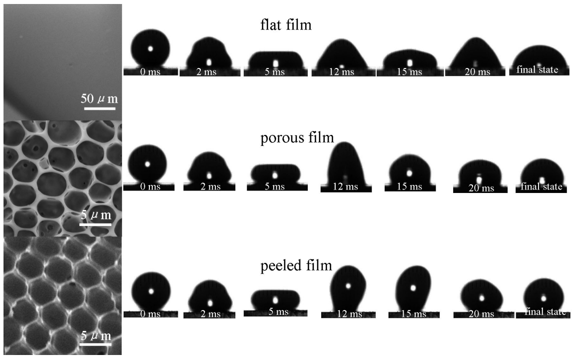

The peeled film obtained on the isopropanol substrate through breath figure method exhibits best hydrophobic property, and the water droplet impact behavior shows obvious rebound tendency and the weak maximum spreading diameter.